

# 1. Two level system (Landau-Zener)

*January 5, 2022*

*Jan Strleček*

Let's have a Hamiltonian

$$\hat{H}(t) = \begin{pmatrix} \Omega(t) & \Delta(t) \\ \Delta(t) & -\Omega(t) \end{pmatrix} \quad (1.1)$$

for  $\Omega : \mathbb{R}^+ \rightarrow \mathbb{R}$ ,  $\Delta : \mathbb{R}^+ \rightarrow \mathbb{R}$ . Its spectrum is

$$E_1(t) = -E_0(t) = \sqrt{\Omega^2(t) + \Delta^2(t)} \quad (1.2)$$

and eigenvectors

$$|0(t)\rangle = \mathcal{N}_+ \begin{pmatrix} \frac{E_0(t)+\Omega(t)}{\Delta(t)} \\ 1 \end{pmatrix}; \quad |1(t)\rangle = \mathcal{N}_- \begin{pmatrix} \frac{E_1(t)+\Omega(t)}{\Delta(t)} \\ 1 \end{pmatrix} \quad (1.3)$$

for normalization constants  $N_\pm = \left( \frac{\pm E_0(t) + \Omega(t)}{\Delta(t)} + 1 \right)^{-1/2}$ .

The goal will be to find *fidelity*  $F := |\langle 0(t) | \psi(t) \rangle|^2$  of different driving protocols. For this we need to solve time Schrödinger equation

$$\hat{H}(t) |\psi(t)\rangle = i \frac{d}{dt} |\psi(t)\rangle \quad (1.4)$$

with time varying Hamiltonian. For 2-dimentional system with  $|\psi(t)\rangle =: (a(t), b(t))$  we get system of *two coupled differentials equations of the 1. order with non-constant coefficients*

$$\Omega(t)a(t) + \Delta(t)b(t) = i\dot{a}(t) \quad (1.5)$$

$$\Delta(t)a(t) - \Omega(t)b(t) = i\dot{b}(t) \quad (1.6)$$

with normalization

$$a^2(t) + b^2(t) = 1, \quad \forall t \in [0, T_f]. \quad (1.7)$$

## 1.0.1 Harmonic oscillator correspondence

The Equations 1.5, 1.6 have no general analytical solution, with the exceptions of a few easy protocols  $\hat{H}(t)$ . Those equations can be rewritten to *one differential equation of 2. order with non-constant coefficients*, which can be rewritten in a form of a *damped harmonic oscillator without external force*

$$0 = \ddot{a}(t) + \gamma(t)\dot{a}(t) + \omega^2(t)a(t) \quad (1.8)$$

$$\gamma(t) := i\Omega(t)(1 - \Delta(t)) - \frac{\dot{\Delta}(t)}{\Delta(t)} \quad (1.9)$$

$$\omega^2(t) := i\dot{\Omega}(t) - i\Omega(t)\frac{\dot{\Delta}(t)}{\Delta(t)} - \Delta(t)\Omega^2(t). \quad (1.10)$$

Along with the normalization condition 1.7, this solves the Schrödinger equation. Note that in this form  $\Delta \neq 0$ , but we can switch role of  $\Delta$  and  $\Omega$  driving due to system symmetry and the fidelity will be unchanged.

The solution of Eq. 1.8 leads to damped oscillations. This characteristic will propagate to the solution for fidelity.

### Classical mechanics correspondence

From the perspective of classical mechanics, meaning  $x(t)$  is a position in a phase space  $(\mathbf{x}, \mathbf{p})$ , we can write classical Lagrangian from Eq. 1.8 as

$$\mathcal{L} = \frac{1}{2} \exp \left( \int_0^t \gamma(s) ds \right) (\dot{x}^2 - \omega^2(t)x^2) \quad (1.11)$$

*Proof.* The correspondence of Lagrangian 1.11 with Eq. 1.8 can be shown by direct evaluation of Euler-Lagrange equations

$$\begin{aligned} \frac{\partial \mathcal{L}}{\partial x} - \frac{d}{dt} \frac{\partial \mathcal{L}}{\partial \dot{x}} &= 0 \\ \frac{1}{2} \exp \left( \int_0^t \gamma(s) ds \right) (-2\omega^2(t)x) - \frac{d}{dt} \left( \exp \left( \int_0^t \gamma(s) ds \right) \dot{x} \right) &= 0 \\ -\omega^2(t)x - \gamma(t)\dot{x} - \ddot{x} &= 0, \end{aligned} \quad (1.12)$$

where derivation along upper bound  $F(x) := \int_0^{g(x)} f(t) dt \Rightarrow F'(x) = f(g(x))g'(x)$  for  $f(x) \in L^1(0, g(x))$  and differentiable function  $g$ , was used.  $\square$

## 1.1 Geodesical driving

As was mentioned, the Schrödinger equation has no general analytical solution, except a few easy protocols  $\hat{H}(t)$ . One of them is *Geodesical protocol*.

Define driving in 3-dimensional space (the reason will be the urge to rewrite it using  $\hat{\sigma}$  matrices)

$$d(t) \equiv \begin{pmatrix} \Omega(t) \\ \Xi(t) \\ \Delta(t) \end{pmatrix} := \begin{pmatrix} -s \cos(\omega(T_f)t) \\ 0 \\ s \sin(\omega(T_f)t) \end{pmatrix} \quad (1.13)$$

parametrized by time  $t \in [0, 1]$  and with use of *speed regulating function*  $\omega(T_f) := \pi/T_f$ . This means, the driving will always be along half-sphere, as in Fig. 1.8.

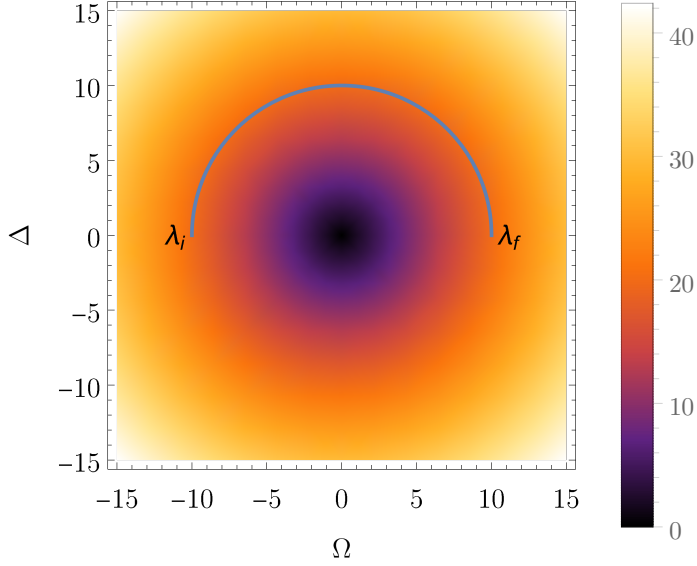


Figure 1.1: Driving along the geodesic.  $\lambda_i$  and  $\lambda_f$  are initial resp. final parameters. DensityPlot shows the difference between Hamiltonian eigenvalues.

### 1.1.1 Derivation of the fidelity

Because the Hamiltonian can be rewritten using Pauli matrices

$$\hat{H}(t) = \begin{pmatrix} -s \cos(t\omega) & s \sin(t\omega) \\ s \sin(t\omega) & s \cos(t\omega) \end{pmatrix} = \Delta(t)\sigma_x + \Omega(t)\sigma_z = d(t).\hat{\sigma} \quad (1.14)$$

one can see that changing from the [original frame](#) to [moving frame](#) of reference (let's omit the final time dependence  $\omega = \omega(T_f)$  for a while)

$$\psi(t) =: e^{\frac{i\omega}{2}\hat{\sigma}_y t} \tilde{\psi}(t) \quad (1.15)$$

reflects rotational symmetry of the problem. This change of reference frame transforms Schrödinger equation

$$\begin{aligned} \hat{H}(t)\psi(t) &= i\psi'(t) \\ \hat{H}(t)e^{\frac{i\omega}{2}\hat{\sigma}_y t}\tilde{\psi}(t) &= ie^{\frac{i\omega}{2}\hat{\sigma}_y t} \left( \frac{i\omega\hat{\sigma}_y}{2} \right) \tilde{\psi}(t) + ie^{\frac{i\omega}{2}\hat{\sigma}_y t} \tilde{\psi}'(t) \\ \underbrace{\left( e^{-\frac{i\omega}{2}\hat{\sigma}_y t} \hat{H}(t) e^{\frac{i\omega}{2}\hat{\sigma}_y t} + \frac{\omega}{2} \hat{\sigma}_y \right)}_{\tilde{H}(t)} \tilde{\psi}(t) &= i\tilde{\psi}'(t). \end{aligned} \quad (1.16)$$

Therefore we can equivalently solve the Fidelity problem in this new coordinate system.

Hamiltonian in the moving frame is

$$\tilde{H} = \begin{pmatrix} -s & -i\omega(T_f)/2 \\ i\omega(T_f)/2 & s \end{pmatrix}, \quad (1.17)$$

which is time independent. The Schrödinger equation can now be easily solved using evolution operator

$$\hat{U}(t) = e^{-i\tilde{\hat{H}}t} = \begin{pmatrix} \cos\left(\frac{t}{2}q(T_f)\right) + \frac{2is\sin\left(\frac{t}{2}q(T_f)\right)}{q(T_f)} & -\frac{\omega(T_f)\sin\left(\frac{t}{2}q(T_f)\right)}{q(T_f)} \\ \frac{\omega(T_f)\sin\left(\frac{t}{2}q(T_f)\right)}{q(T_f)} & \cos\left(\frac{t}{2}q(T_f)\right) - \frac{2is\sin\left(\frac{t}{2}q(T_f)\right)}{q(T_f)} \end{pmatrix}, \quad (1.18)$$

for  $q(T_f) = \sqrt{4s^2 + \omega(T_f)^2}$ .

In the original frame we get the evolution of the state  $\psi(0)$

$$\psi(t) = e^{\frac{i\omega}{2}\hat{\sigma}_y t} \hat{U}(t) \tilde{\psi}(0) = \underbrace{e^{\frac{i\omega}{2}\hat{\sigma}_y t} \hat{U}}_{\hat{U}(t)} \underbrace{e^{-\frac{i\omega}{2}\hat{\sigma}_y t} \tilde{\psi}(0)}_{\psi(0)}. \quad (1.19)$$

Then the evolved wavefunction is

$$|\psi(t)\rangle = \begin{pmatrix} \cos\left(\frac{t}{2}q(T_f)\right) + \frac{2is\cos(t\omega(T_f))\sin\left(\frac{t}{2}q(T_f)\right)}{q(T_f)} \\ \frac{(\omega(T_f) - 2is\sin(t\omega(T_f)))\sin\left(\frac{t}{2}q(T_f)\right)}{q(T_f)} \end{pmatrix} \quad (1.20)$$

and the ground state

$$|0(t)\rangle = \mathcal{N} \begin{pmatrix} -\cot\left(\frac{t}{2}\omega(T_f)\right) \\ 1 \end{pmatrix}, \quad (1.21)$$

for a normalization constant  $\mathcal{N} := |\langle 0(t)|0(t)\rangle|^{-1}$ . Fidelity during the transport is then<sup>1</sup>

$$F = |\langle 0(t)|\psi(t)\rangle|^2, \quad (1.22)$$

An explicit formula for fidelity in time  $t$  and geodesic driving with final time  $T_f$  is then

$$F(t, T_f) = \frac{\pi^2 \left( \cos\left(t\sqrt{\frac{\pi^2}{T_f^2} + 4s^2}\right) + 1 \right) + 8s^2 T_f^2}{2 \sin^4\left(\frac{\pi t}{2T_f}\right) \left(4s^2 T_f^2 + \pi^2\right) \left(\left|\cot\left(\frac{\pi t}{2T_f}\right)\right|^2 + 1\right)^2}. \quad (1.23)$$

The domain can be extended to  $t \in [0, T_f]$ ,  $T_f \in [0, \infty]$  because

$$\lim_{t \rightarrow 0} F = 1, \quad \lim_{T_f \rightarrow 0} F = 0.$$

Sometimes the *Infidelity*, defined as  $I := 1 - F$ , will be used. Its meaning is the *probability of excitation of the state*.

---

<sup>1</sup>If we would calculate the fidelity in the **comoving frame**, we would get exactly one. This is the essence of counterdiabatic driving.

### 1.1.2 Analysis of the infidelity formula

Fidelity for some fixed final time is just oscillating curve close to 1. For  $T_f = 10$  it can be seen on Fig. 1.2. The *final fidelity* (at  $t = T_f$ ) dependence on final time  $T_f$  can be seen on Fig. 1.3 and 1.4.

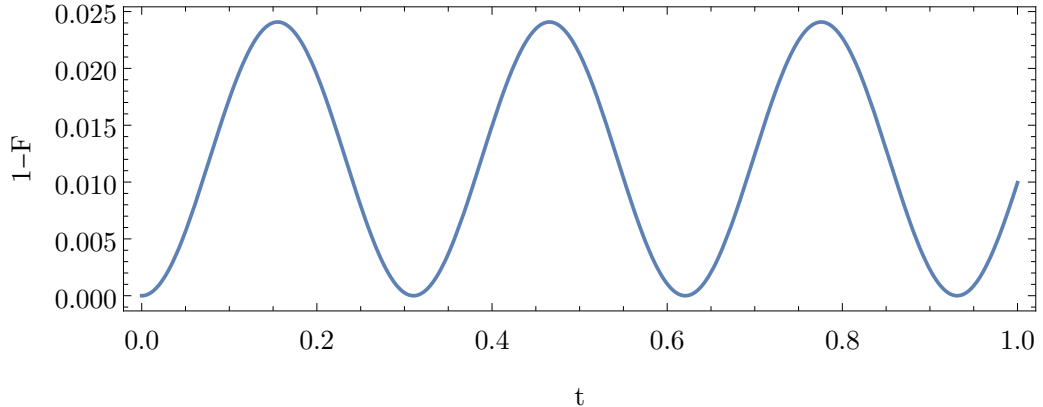


Figure 1.2: Infidelity in time for final time  $T_f = 1$  for geodesical driving.

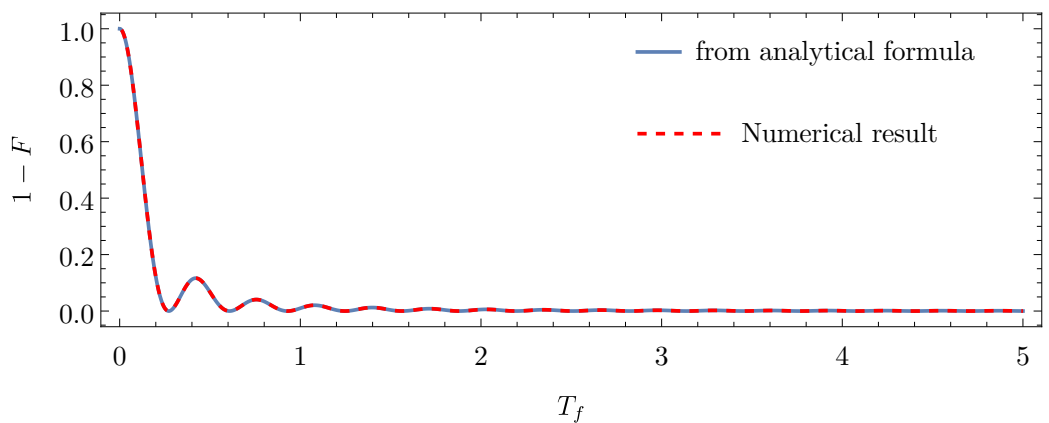


Figure 1.3: Final infidelity dependence on final time  $T_f$  for geodesical driving.

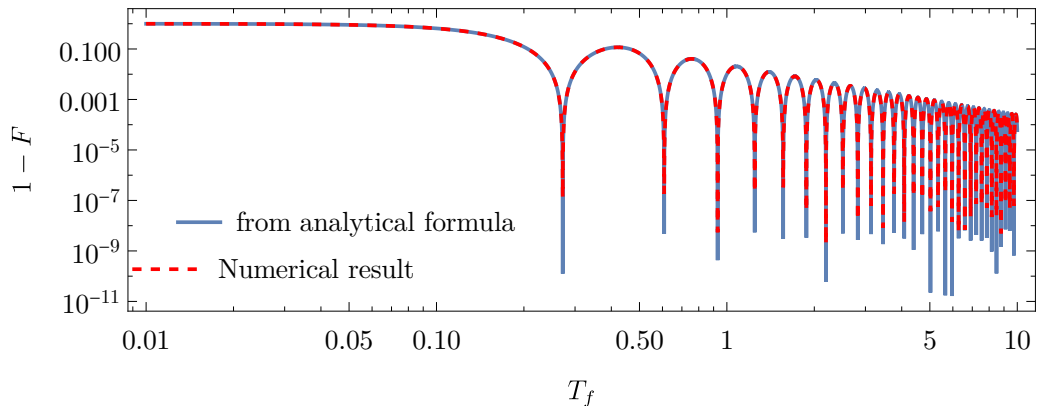


Figure 1.4: Infidelity dependence on final time in log-log scale. We can observe difference in numerical evaluation of different firmulas in the height of spikes.

From the fidelity Eq. 1.23 goes that  $F = 1$  is equivalent to

$$\cos\left(\sqrt{T_s^2 + \pi^2}\right) = 1, \quad (1.24)$$

for  $T_s := 2sT_f$ . The solution to this equation is

$$T_s = \sqrt{(2\pi k)^2 - \pi^2} \text{ for } k \in \mathbb{N}. \quad (1.25)$$

This can be checked numerically, see Fig. 1.5. Because  $F = 1$  has solutions 1.25, its dependence on final time in logarithmic scale has spikes going to 0, see Fig. 1.4, and their density is linear in  $T_f$ .

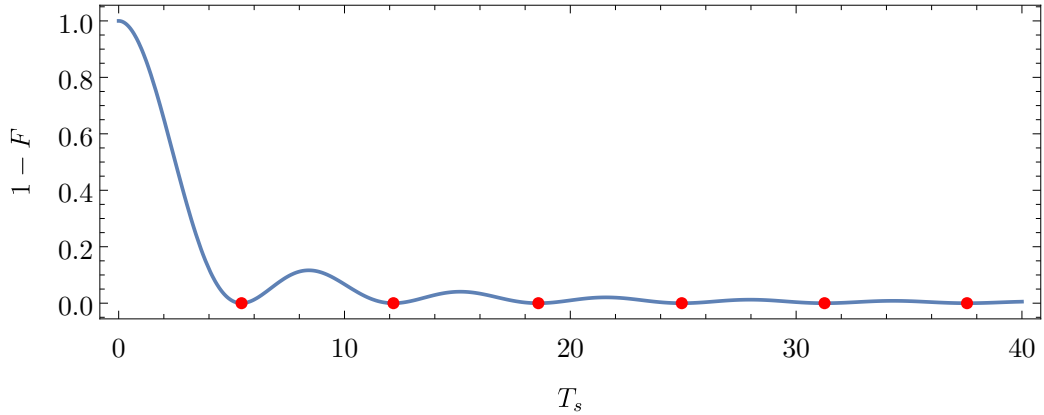


Figure 1.5: Rescaled final infidelity  $T_s := 2sT_f$  dependence on final time. Red points are for  $F = 1$ .

Fidelity as a function of time and final time can be seen in Figures 1.6. Note that only  $t < T_f$  has physical meaning.

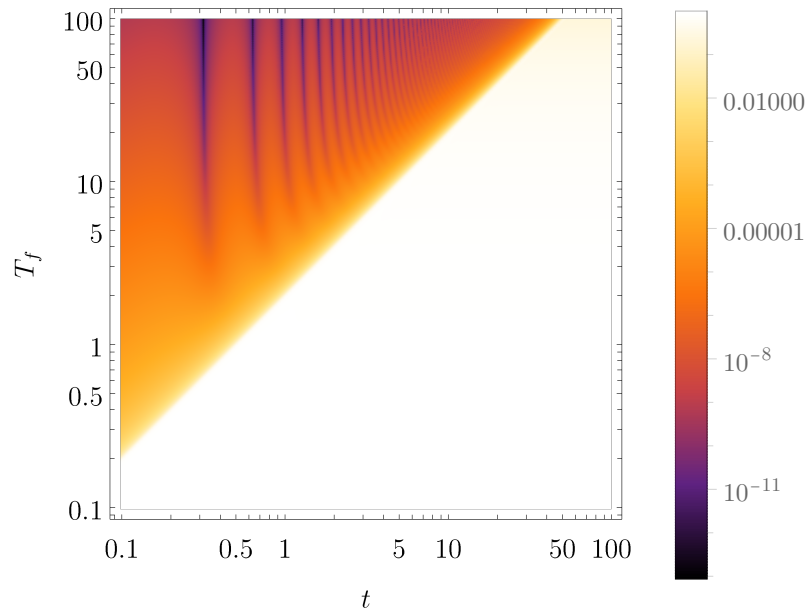


Figure 1.6: Fidelity dependence on time and final time in log log scale. Note that only  $t < T_f$  has physical meaning.

### 1.1.3 Energy variance

Evaluating the fidelity for geodesical driving gives a function of time  $t$  and final time  $T_f$

$$\begin{aligned} \delta E^2 = & \frac{s^2}{2q^2} \left[ \left[ 16s^4 + 2s^2 \left( (\omega^2 - 8s^2) \cos(2t\omega) - 8\omega^2 \cos^2(t\omega) \cos(t\sqrt{q}) \right) \right. \right. \\ & + 14s^2\omega^2 + \omega^4 \Big] - \omega^2 \left( (2s^2 + \omega^2) \cos(2t\omega) - 2s^2 \right) \cos(2tq) \\ & \left. \left. + 8s^2\omega q \sin(2t\omega) \sin(tq) + \omega^3 q \sin(2t\omega) \sin(2tq) \right], \right] \end{aligned} \quad (1.26)$$

see the definition of  $q$  under Eq. 1.18. Its value as can be seen on Fig. 1.7. Note that only  $t < T_f$  has a physical meaning, therefore the dependence is smooth along the whole geodesical driving protocols.

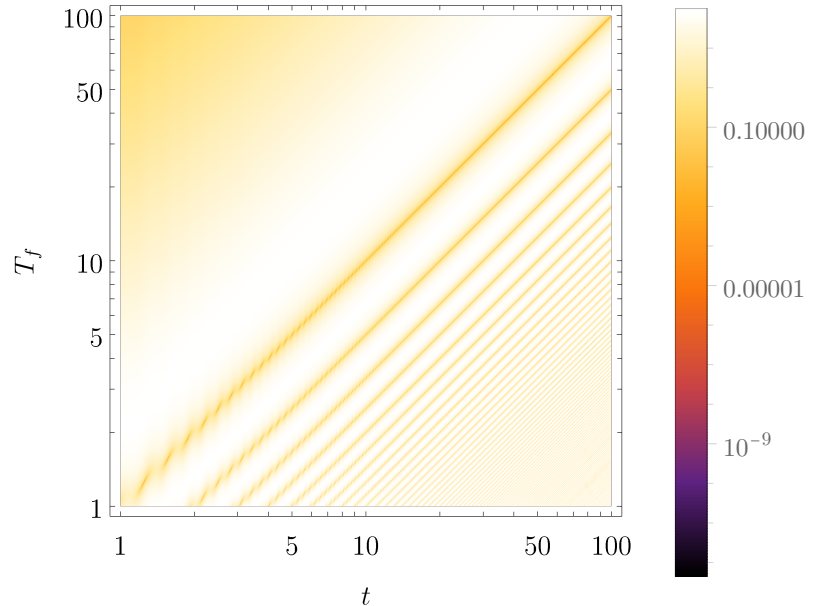


Figure 1.7: Energy variance for geodesical driving protocol.

## 1.2 Linear driving

In this case we define the driving as

$$\Omega(t) = \Omega_{sc} \left( \frac{2t}{T_f} - 1 \right), \quad \Delta(t) = \Delta_{sc}, \quad \text{for } \Omega_{sc} = 10, \Delta_{sc} = 0.3 \quad (1.27)$$

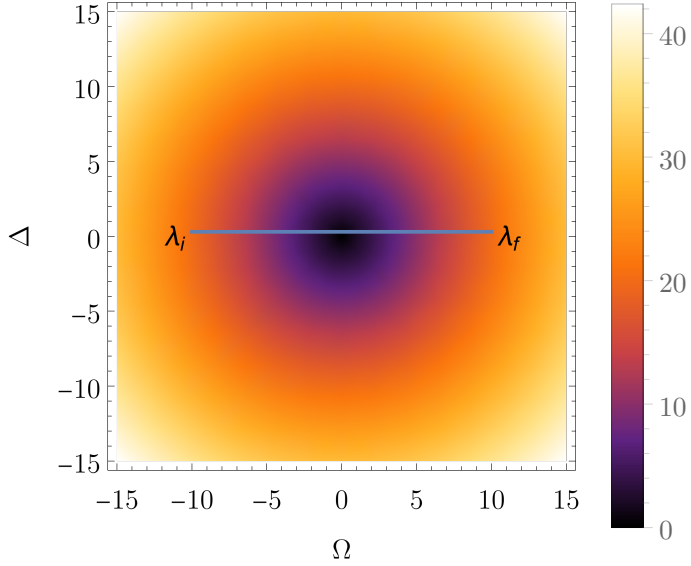


Figure 1.8: Driving along the linear path.  $\lambda_i = (-10; 0.3)$  and  $\lambda_f = (10; 0.3)$  are initial resp. final parameters. DensityPlot shows the difference between Hamiltonian eigenvalues.

### 1.2.1 Dependence on time

The fidelity in time can be seen on Fig. 1.9. We can see that for  $t \approx T_f/2$  Hamiltonian parameters change quickly leading to the fast state excitation. Then the Harmonic oscillator damping of Schrödinger equation gets involved, and oscillations are quickly going to zero, never disappearing entirely.

We can see that the final fidelity decreases with longer final time, which correctly leads to adiabatic driving  $\lim_{T_f \rightarrow \infty} F = 0$ . For short final times we can observe so called quench,  $\lim_{T_f \rightarrow 0} F = 1$ . The important phenomenon on this image are the oscillations around  $t = T_f/2$ , which are increasing with  $T_f$ .

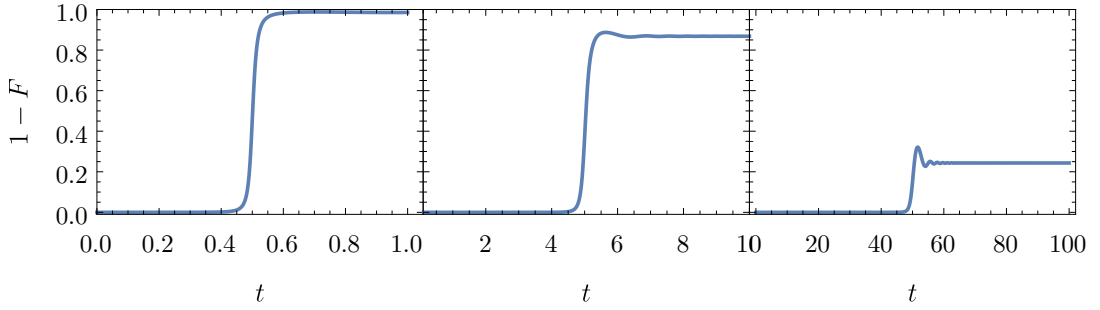


Figure 1.9: Infidelity in time for three final times  $T_f \in \{1, 10, 100\}$  for linear driving.

If the driving is slow enough (meaning of this will be clear later on), the final fidelity will oscillate between 0 and some small value, see Fig. 1.10. Because the eigenstate  $|0(t)\rangle = \begin{pmatrix} 1 & 0 \end{pmatrix}$ , the frequency of oscillations in fidelity is the same as oscillations in  $a(t)$  in Eq. 1.10. For the linear driving this is

$$\omega^2(t) = \frac{2i}{T_f} \Omega_{sc} - \Delta_{sc} \Omega_{sc}^2 \left( \frac{2t}{T_f} - 1 \right)^2. \quad (1.28)$$

This means the frequency is linear in time and has a square root dependence on  $\Delta$ .

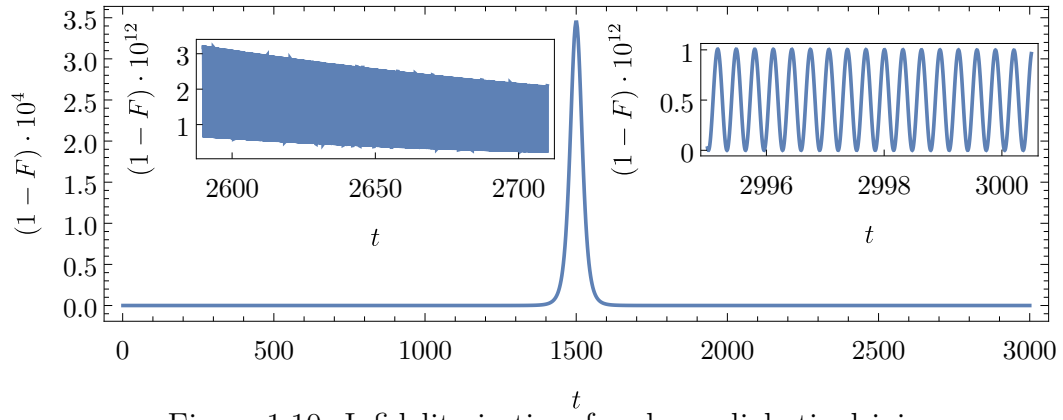


Figure 1.10: Infidelity in time for close adiabatic driving.

### 1.2.2 Dependence on final time

Because the oscillations after fast parameter change in the Hamiltonian never disappear entirely, we must observe those oscillations even at the final time. Final fidelity (meaning the fidelity at final time  $F(T_f)$ ) has dependence on  $T_f$  as can be seen in Fig. 1.11. Because after the final time  $T_f \approx 2000$  the values are so small, we can observe some fine structure of the fidelity, along with numerical error artifacts.

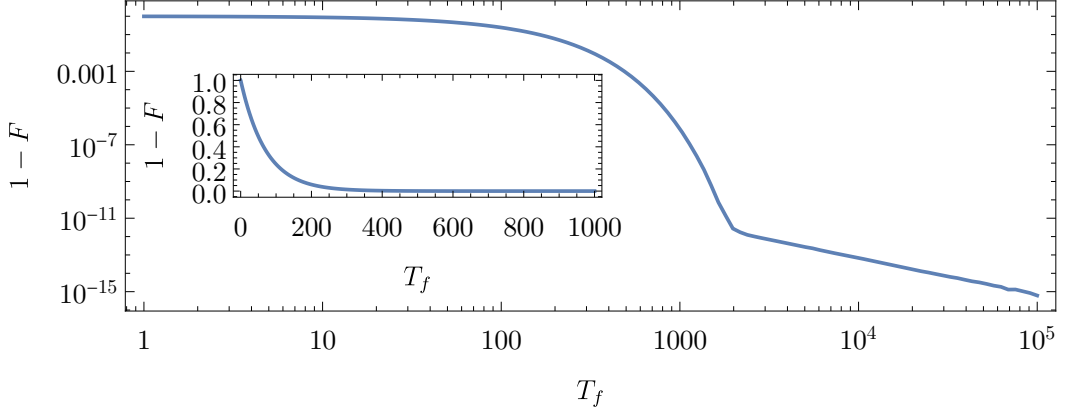


Figure 1.11: Final infidelity as a function of  $T_f$ .

The important question is now: "what is numerical error and what is remnant of oscillations?" The answer is not so simple, but we can make few statements. First of all, the numerical precision of this calculation was found to be around  $10^{-14}$ . This can be seen when we zoom at the edge of *smooth* and *chaotic* part of the plot, see Fig ??<sup>2</sup>. This means that there are oscillations are of physical origin. Those small oscillations are the remnants of the big oscillations after fast fidelity change, see Fig. 1.9. We can eliminate the effect of these oscillations and see the *average final infidelity*, defined as

$$\langle 1 - F \rangle_a(T_f) := \frac{1}{(1-a)T_f} \int_{aT_f}^{T_f} F(t) dt. \quad (1.29)$$

If we average the fidelity on interval  $(0.9T_f, T_f)$  (getting  $\langle 1 - F \rangle_{0.9}$ ), we get the same result as for  $\langle 1 - F \rangle_{0.99}$ . See Fig. 1.12.

Then we can split the driving to three regimes:

- *exponential/fast-driving regime* –  $(1 - F) = \langle 1 - F \rangle_a = \exp(-\xi T_f)$ ,  $\xi \in \mathbb{R}^+$
- *transitional regime* – the infidelity dependence is oscillatory and has no simple prescription
- *polynomial/adiabatic regime* –  $\langle 1 - F \rangle_a \propto T_f^{-\kappa}$  for  $\kappa \in \mathbb{R}^+$ ,  $a \in [0.6T_f, 0.999T_f]$ .

Two questions now arise. What are the coefficients  $\xi$  and  $\kappa$  and on which intervals in  $T_f$  they hold? Let's answer them one by one.

---

<sup>2</sup>First zero probably appears at 1889, which is the same year when the Eiffel tower was officially opened, or the year when the first Juke box goes into operation in San Francisco.

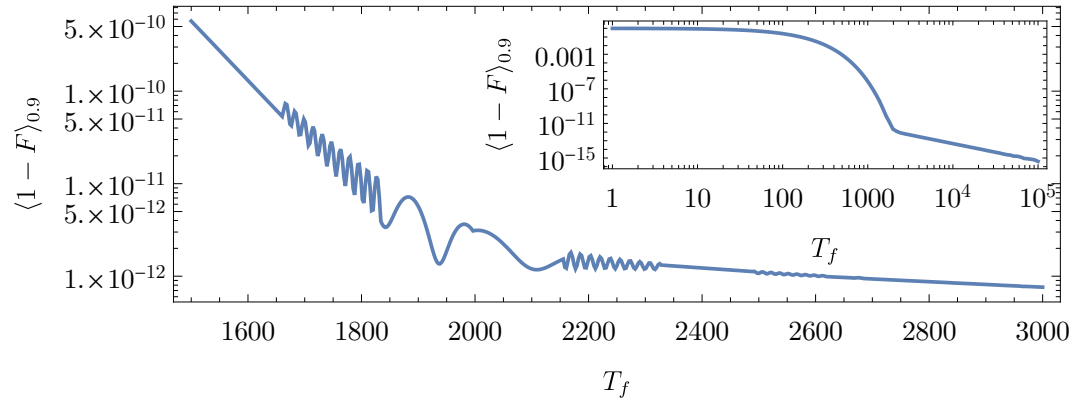


Figure 1.12: Final infidelity as a function of  $T_f$ . Detail on the edge between *smooth* and *chaotic* regimes.

### 1.2.3 Transition between the fast-driving and adiabatic regime

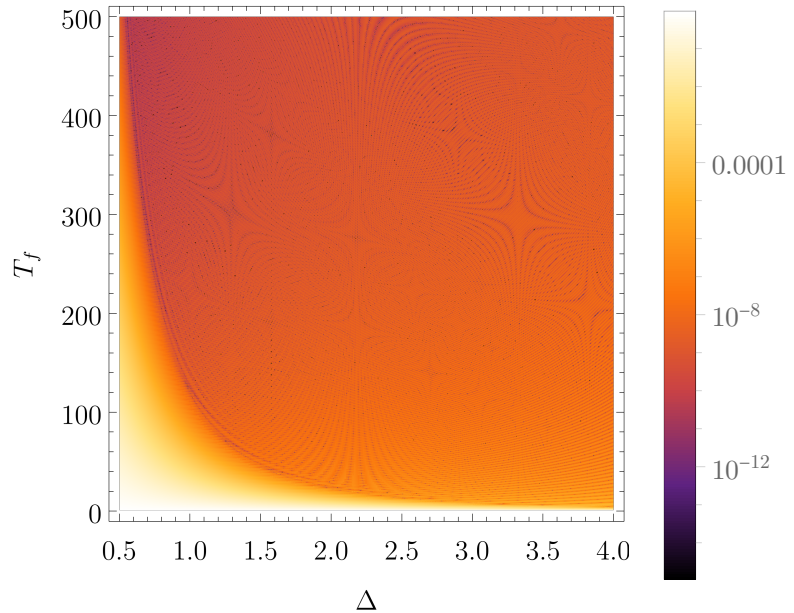


Figure 1.13: Final infidelity as a function of  $\Delta$  and  $T_f$  and its three regimes. Zoomed boundary between them can be seen on 1.14.

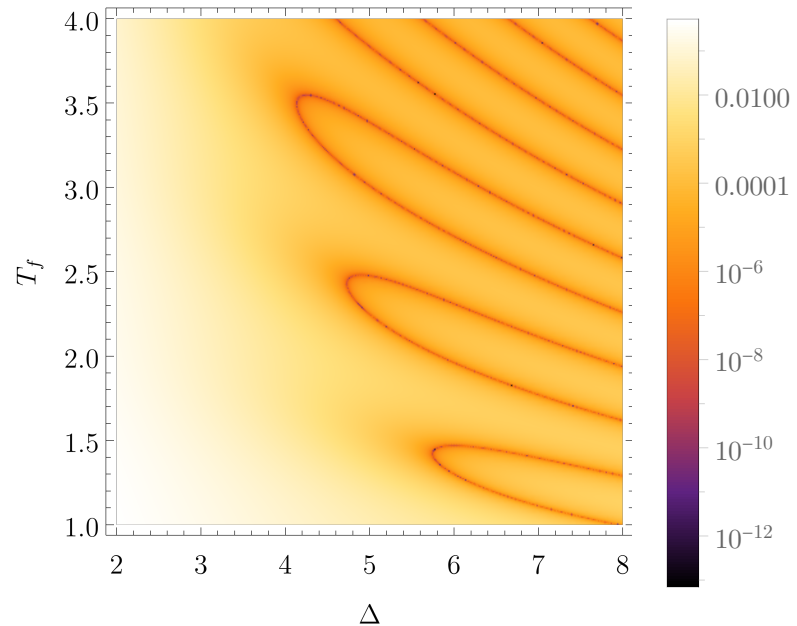


Figure 1.14: Fine structure of the boundary between fast-driving and adiabatic regimes of final infidelity.

#### 1.2.4 Coefficients $\xi$ and $\kappa$

### 1.2.5 Energy variance

Energy variance resembles structure similar to fidelity. Compare Fig. 1.15 with 1.6.

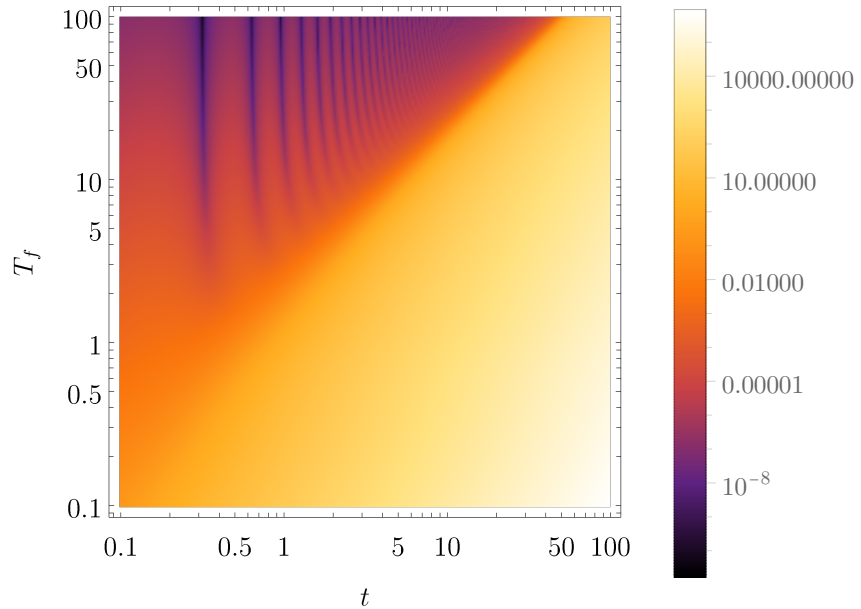


Figure 1.15: Energy variance for  $\Omega = 0.2$  for linear driving. Note that only  $t < T_f$  has physical meaning.

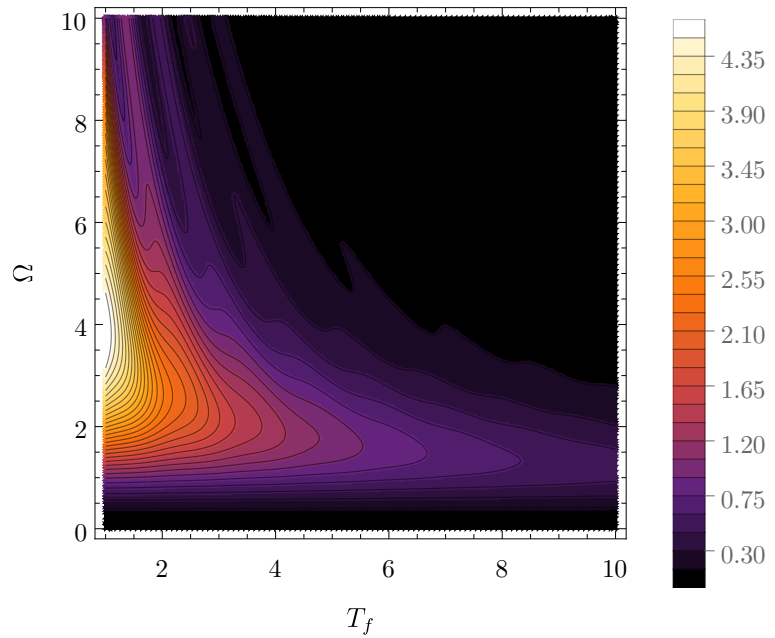


Figure 1.16: Energy variance for  $t = T_f/2$  for linear driving.

### 1.3 Energy variance for two level system

For two level system, the variance

$$\delta E^2(t) := \langle \psi(t) | \hat{H}^2 | \psi(t) \rangle - \langle \psi(t) | \hat{H} | \psi(t) \rangle^2 \quad (1.30)$$

can be rewritten inserting identity  $\mathbb{1} = |0\rangle\langle 0| + |1\rangle\langle 1|$  around Hamiltonian. Omitting the time dependence of every element we get

$$\begin{aligned} \delta E^2 &= \langle \psi | \mathbb{1} \hat{H}^2 \mathbb{1} | \psi \rangle - \langle \psi | \mathbb{1} \hat{H} \mathbb{1} | \psi \rangle^2 \\ &= \langle \psi | 0 \rangle \langle 0 | \hat{H}^2 | 0 \rangle \langle 0 | \psi \rangle + \langle \psi | 1 \rangle \langle 1 | \hat{H}^2 | 1 \rangle \langle 1 | \psi \rangle \\ &\quad + \langle \psi | 0 \rangle \langle 0 | \hat{H}^2 | 1 \rangle \langle 1 | \psi \rangle + \langle \psi | 1 \rangle \langle 1 | \hat{H}^2 | 0 \rangle \langle 0 | \psi \rangle \\ &\quad - \left( \langle \psi | 0 \rangle \langle 0 | \hat{H} | 0 \rangle \langle 0 | \psi \rangle + \langle \psi | 1 \rangle \langle 1 | \hat{H} | 1 \rangle \langle 1 | \psi \rangle \right. \\ &\quad \left. + \langle \psi | 0 \rangle \underbrace{\langle 0 | \hat{H} | 1 \rangle}_{\propto \langle 0 | 1 \rangle = 0} \langle 1 | \psi \rangle + \langle \psi | 1 \rangle \underbrace{\langle 1 | \hat{H} | 0 \rangle}_{\propto \langle 0 | 1 \rangle = 0} \langle 0 | \psi \rangle \right)^2. \end{aligned} \quad (1.31)$$

Using Fidelity definition  $F(t) = |\langle 0(t) | \psi(t) \rangle|^2$  and Schrödinger equation  $\hat{H} |k\rangle = E_k |k\rangle$  we have

$$\delta E^2 = F E_0^2 + (1 - F) E_1^2 - (F E_0 + (1 - F) E_1)^2 = F(1 - F)(E_0 - E_1)^2. \quad (1.32)$$

For three level system we have  $\mathbb{1} = |0\rangle\langle 0| + |1\rangle\langle 1| + |2\rangle\langle 2|$  and

$$\delta E^2 = \sum_{k=1}^3 E_k^2 F_k (1 - F_k) - 4 \prod_{k=1}^3 E_k F_k - 2 F_0 F_1 E_0 E_1 - 2 F_0 F_2 E_0 E_2 - 2 F_1 F_2 E_1 E_2, \quad (1.33)$$

for  $F_k := \langle k | \psi \rangle$ , which has no practical simplification.